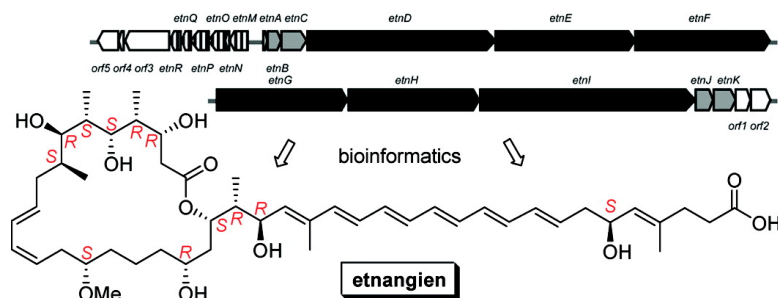


Stereochemical Determination and Complex Biosynthetic Assembly of Etnangien, a Highly Potent RNA Polymerase Inhibitor from the Myxobacterium *Sorangium cellulosum*

Dirk Menche, Fatih Arikan, Olena Perlova, Nicole Horstmann, Wiebke Ahlbrecht, Silke C. Wenzel, Rolf Jansen, Herbert Irschik, and Rolf Müller

J. Am. Chem. Soc., **2008**, 130 (43), 14234-14243 • DOI: 10.1021/ja804194c • Publication Date (Web): 01 October 2008

Downloaded from <http://pubs.acs.org> on February 8, 2009



More About This Article

Additional resources and features associated with this article are available within the HTML version:

- Supporting Information
- Access to high resolution figures
- Links to articles and content related to this article
- Copyright permission to reproduce figures and/or text from this article

[View the Full Text HTML](#)



ACS Publications
 High quality. High impact.

Stereochemical Determination and Complex Biosynthetic Assembly of Etnangien, a Highly Potent RNA Polymerase Inhibitor from the Myxobacterium *Sorangium cellulosum*

Dirk Menche,^{*,†,‡} Fatih Arikan,[‡] Olena Perlova,[‡] Nicole Horstmann,[‡] Wiebke Ahlbrecht,[†] Silke C. Wenzel,[‡] Rolf Jansen,[§] Herbert Irschik,[§] and Rolf Müller^{*,§,⊥}

University of Heidelberg, Department of Organic Chemistry, INF 270, D-69120 Heidelberg, Germany, Helmholtz Centre for Infection Research (HZI), Medicinal Chemistry, Inhoffenstrasse 7, D-38124 Braunschweig, Germany, Helmholtz Centre for Infection Research (HZI), Microbial Drugs and Saarland University, Pharmaceutical Biotechnology, P.O. Box 151150, D-66041 Saarbrücken, Germany

Received June 3, 2008; E-mail: dirk.menche@oci.uni-heidelberg.de; rom@mx.uni-saarland.de

Abstract: A potent novel analogue of the natural macrolide antibiotic etnangien, a structurally unique RNA polymerase inhibitor from myxobacteria, is reported. It may be readily obtained from fermentation broths of *Sorangium cellulosum* and shows high antibiotic activity, comparable to that of etnangien. However, it is much more readily available than the notoriously labile authentic natural product itself. Importantly, it is stable under neutral conditions, allowing for elaborate NMR measurements for assignment of the 12 hydroxyl- and methyl-bearing stereogenic centers. The full absolute and relative stereochemistries of these complex polyketides were determined by a combination of extensive high-field NMR studies, including *J*-based configuration analysis, molecular modeling, and synthetic derivatization in combination with an innovative method based on biosynthetic studies of this polyketide which is also presented here. A first look into the solution conformation and 3D structure of these promising macrolide antibiotics is reported. Finally, the complete biosynthetic gene cluster was analyzed in detail, revealing a highly unusual and complex *trans*-AT type polyketide biosynthesis, which does not follow colinearity rules, most likely performs programmed iteration as well as module skipping, and exhibits HMG-CoA box-directed methylation.

Introduction

Bacterial DNA-dependent RNA polymerase presents an attractive drug target for the development of novel antibiotics as RNA chain elongation is essential for bacterial growth.^{1–3} The molecular structure and role of this protein are increasingly well understood,⁴ which enables a perception of inhibitor–target interaction on the molecular level and adds to the attractiveness for inhibitor design.⁵ So far, the rifamycins are the only class of clinically used RNA polymerase inhibitors. However, resistance has been increasingly emerging which renders the

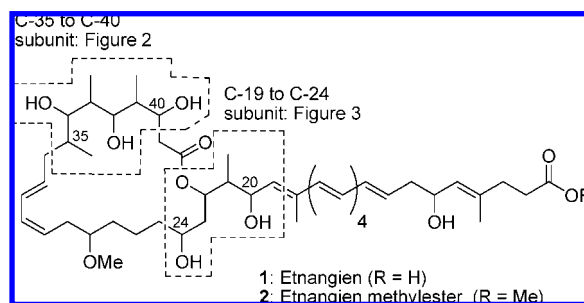


Figure 1. Planar structure of etnangien (1).

development of novel types of RNA polymerase inhibitors an important research goal.⁶

The polyketide natural product etnangien (1, Figure 1), originally isolated from the myxobacterium *Sorangium cellulosum*, strain So ce750, later from So ce1045, constitutes a new structural type of a particularly efficient RNA polymerase inhibitor *in vitro* and *in vivo*.⁷ It is effective against a broad panel of Gram-positive bacteria, especially those belonging to the actinomycetes. In addition, it appears to exhibit no cross-resistance to rifampicin. Furthermore, it also retains activity

[†] University of Heidelberg.

[‡] HZI: Medicinal Chemistry.

[§] HZI: Microbial Drugs.

[⊥] Saarland University.

- (1) Das, A.; DeVito, J.; Sparkowski, J.; Warren, F. In *Emerging Targets in Antibacterial and Antifungal Chemotherapy*; Sutcliffe, J., Georgopadakou, N. H., Eds.; Chapman and Hall: New York, 1992; pp 68–116.
- (2) Jin, D. J.; Zhou, Y. N. *Methods Enzymol.* **1996**, *273*, 300–319.
- (3) O'Neill, A.; Oliva, B.; Storey, C.; Hoyle, A.; Fishwick, C.; Chopra, I. *Antimicrob. Agents Chemother.* **2000**, *44*, 3163–3166.
- (4) Zhang, G.; Campbell, E. A.; Minakhin, L.; Richter, C.; Severinov, K.; Darst, S. A. *Cell* **1999**, *98*, 811–824.
- (5) Campbell, E. A.; Pavlova, O.; Zenkin, N.; Leon, F.; Irschik, H.; Jansen, R.; Severinov, K.; Darst, S. A. *EMBO J.* **2005**, *24*, 674–682.

- (6) Parenti, F.; Lancini, G. In *Antibiotic and Chemotherapy*; O'Grady, F., Lambert, H. P., Finch, R. G., Greenwood, D., Eds.; Churchill Livingstone: New York, 1997; pp 453–459.

against retroviral DNA polymerase and shows only low cytotoxicity against mammalian cell cultures, which adds to the attractiveness for further development. However, preclinical advancement is severely hampered by the notorious instability of etnangien (**1**), which is intrinsically associated with the polyene side chain in combination with the acid functionality at C-1. Consequently, no structure–activity relationship (SAR) data are available so far. Herein, we disclose the first analogue of etnangien, the methyl ester **2**, and report a very convenient and efficient procedure for its preparation directly from the crude extract of the myxobacterium *S. cellulosum*. Etnangien methyl ester (**2**) retains the biological potency of etnangien (**1**). However, it is much more readily available and stable under neutral conditions. On the basis of the stereochemically identical methyl ester we report the configurational determination of etnangien by extensive high-field NMR experiments in combination with molecular modeling, chemical methods, and an innovative procedure utilizing the predictability of the stereochemistry based on biosynthetic analyses. Finally, a biosynthetic model for this structurally unique secondary metabolite is reported, which entails a highly unusual gene cluster.

Results and Discussion

A Potent Stable Analogue. *Sorangium cellulosum* strain So ce1045, was identified in a screening for an efficient etnangien-producing strain to enable this first analogue study. After optimizing cultivation conditions, fermentations were performed at 30 °C in a 70-L bioreactor agitated by a circulating pump/stirrer system in the presence of 1% of Amberlite XAD 16 neutral resin for absorption of excreted secondary metabolites. After eight days, HPLC analysis indicated an antibiotic production of 5 mg/L. The adsorber resin and cell mass (335 g) were subsequently harvested by centrifugation and extracted with methanol. Isolation of **1** proceeded according to previously established procedures and included several water/ethyl acetate partitions and RP MPLC using MeOH/NH₄OAc buffer eluents.⁷ In all purification steps, the stabilizer 4-*tert*-butylcatechol has to be present to avoid degradation. By this protocol, 113 mg of etnangien (**1**) were obtained in a mixture with ammonium acetate (determined by ¹H NMR). The spectroscopic data of **1** were identical to those previously reported for etnangien.⁷

In order to mitigate the inherent acid-mediated instability/sensitivity of the polyunsaturated side chain and to circumvent the precarious isolation procedure requiring buffered media due to the acid functionality and stabilizers against oxidation, the methyl ester **2** was devised as a promising analogue. For its preparation, initially from isolated etnangien, diazomethane proved the reagent of choice among those screened in terms of chemical yield and absence of any sign of isomerization along the polyene side chain. For optimum results, the application of freshly prepared reagent solution, which was washed prior to use with pH 9 buffer, was essential to give the methyl ester in a reliable fashion. Subsequently, this protocol was successfully applied directly to the crude fermentation extract of *S. cellulosum*, So ce1045. This extract in turn may be readily obtained from the adsorber resin by a simple extraction with methanol. While, as expected, an excess of the methylating reagent had to be used, conditions could be optimized to allow for selective esterification of etnangien in the extract in the presence of other

Table 1. Antimicrobial Activity of Etnangien Methyl Ester (**2**) in Comparison to that of Etnangien (**1**)

test organisms	MIC (μg/mL)	
	2	1
Gram-Positive Bacteria		
<i>Staphylococcus aureus</i>	2.5	1.0
<i>S. aureus</i> (rifampicin resistant)	3.1	0.62
<i>Bacillus subtilis</i>	20	10
<i>Corynebacterium glutamicum</i> DSM20300	0.24	0.03
<i>Nocardia corallina</i>	0.12	0.12
<i>Micrococcus luteus</i>	0.39	0.06
Gram-Negative Bacterium		
<i>Escherichia coli</i> tol C	>20	>20
Yeast		
<i>Saccharomyces cerevisiae</i>	>40	>40

constituents, i.e. the other major metabolite icumazol.⁸ As monitored by analytical HPLC, conversion proceeded in an essentially quantitative manner. Methyl ester **2** was then isolated by flash chromatography on silica gel (dichloromethane/methanol = 12:1 to 10:1) and subsequent preparative RP HPLC (methanol/water = 79:21). Notably, this procedure circumvents the laborious isolation protocol of the parent natural product. In particular, it does not require buffers or stabilizing agents. Etnangien methyl ester proved to be stable under neutral conditions. In the absence of light, it can be conveniently stored in methanol at room temperature for several months without degradation.

The structure of this first etnangien analogue was suggested to be the methyl ester **2** because of the close similarity of all of spectroscopic data to those of the parent natural product (UV–vis, IR, and ¹H and ¹³C NMR) and confirmed by detailed NMR analysis (i.e., COSY, HMBC, HMQC-interactions).⁷ Ultimately, the preservation of the constitution and configuration was proven by enzyme-catalyzed ester cleavage to give authentic etnangien. The recovered product proved to be chromatographically and spectroscopically identical with the natural product.

The potent antibiotic activity of etnangien based on RNA polymerase inhibition prompted us to likewise analyze its methyl ester. Table 1 summarizes the inhibitory activity of etnangien methyl ester (**2**) on various bacteria in direct comparison to that of the parent natural antibiotic. Etnangien methyl ester was effective against a broad panel of Gram-positive bacteria, including a rifampicin-resistant strain. Significantly, the stabilized analogue **2** is of similar potency against *Nocardia corallina* and only 2–9-fold less potent against other bacteria as compared to **1**. Only low activity was observed against a Gram-negative bacterium and a yeast, which is in agreement with the data of the parent natural product.

Stereochemical Determination. The planar constitution of etnangien (Figure 1) was elucidated by Schummer, Jansen, and Höfle on the basis of NMR data (¹H and ¹³C NMR, COSY and HMQC)⁷ and consists of a 22-membered macrolactone with a diene (3*Z*,32*E*) and a polyunsaturated side chain with seven *trans* configured alkenes and comprises an array of 12 stereogenic centers, which have not been assigned, leaving 2¹² = 4096 possible diastereomers. Optimum ¹H signal dispersion for our *S. cellulosum* derived sample of etnangien methyl ester (**2**) was obtained in acetone-*d*₆ at the highest available field strength (600 MHz) allowing complete assignment of all resonances in the C-35 to C-40 and the C-19 to C-24 subunits. The ³J_{H,H} coupling

(7) (a) Höfle, G.; Reichenbach, H.; Irschik, H.; Schummer, D. German Patent DE 196 30 980 A1:1-7 (5.2), 1998. (b) Irschik, H.; Schummer, D.; Höfle, G.; Reichenbach, H.; Steinmetz, H.; Jansen, R. *J. Nat. Prod.* **2007**, *70*, 1060–1063.

(8) Reichenbach, H. *J. Ind. Microbiol. Biotechnol.* **2001**, *27*, 149–156.

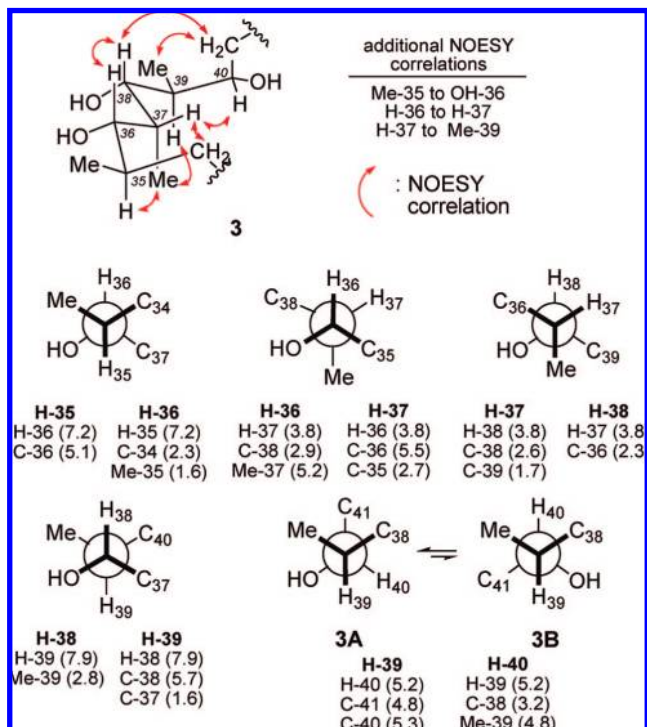


Figure 2. Rotamers determined for the C-35 to C-40 subunit **3** of etnangien methyl ester; coupling constants, $^3J_{H,H}$ and $^{2,3}J_{H,C}$ (Hz) in parentheses.

constants in these regions were extracted from a combination of 2D J -resolved spectra, homonuclear spin decoupling experiments in combination with multiplet analysis,⁹ while measurement of heteronuclear coupling constants ($^{2,3}J_{C,H}$) relied on analysis of HSQC-HECADE spectra.^{10–12} These data suggested the C-19 to C-24 and the C-35 to C-39 regions to be relatively rigid, while a certain degree of flexibility around the (39,40)-bond has to be considered.

The homo- and heteronuclear coupling constants observed for the “northern” C-35 to C-40 subunit **3** of etnangien methyl ester are shown in Figure 2. The available data for the C-35 to C-37 region suggested an all-*syn* relationship between the adjacent methyl and hydroxyl substituents at C-35, C-36, and C-37, by a large homonuclear coupling observed from H-35 to H-36 and a small homonuclear coupling from H-36 to H-37 in combination with small heteronuclear couplings from H-36 to C-34 and Me-35 and from H-37 to C-35. This was further corroborated by large heteronuclear couplings from H-35 to C-36, from H-36 to Me-37, and from H-37 to C-36. A series of NOESY correlations (from H-35 to Me-37, H-37 to H₂-34, Me-35 to OH-36, and H-37 to H-38) confirmed the relative orientation as depicted.

Establishing a relationship between the substituents at C-37 and C-38 relied in a similar fashion on J -based configuration

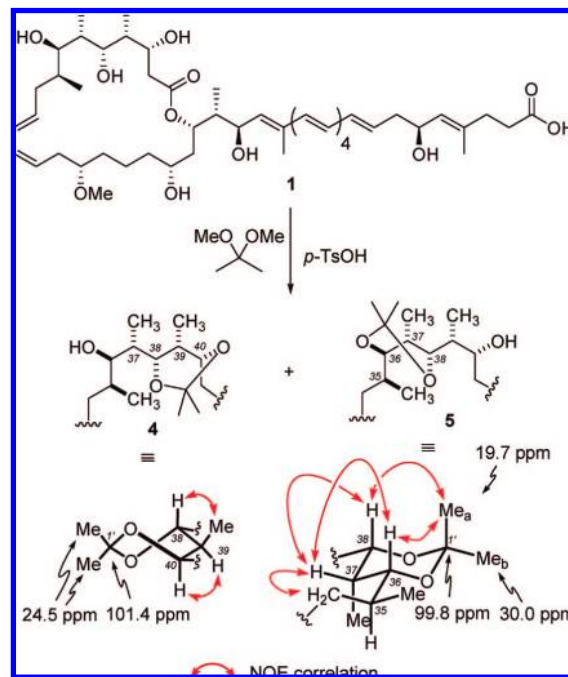


Figure 3. Configurational assignment of the C-35 to C-40 subunit by acetonide formation.

analysis and relevant NOESY correlations. A small homonuclear coupling between H-37 and H-38 and small couplings from H-37 to C-38 and C-39 and from H-38 to C-36 indicated a (37,38)-*syn* relationship. An antiperiplanar relationship between H-38 and H-39 was deduced by a large coupling between these two protons in combination with a small coupling from H-38 to Me-39 and from H-39 to C-37 in combination with a large coupling from H-39 to C-38, suggesting that the C-38 to C-39 subunit resides in the depicted conformation **3**. A key NOESY correlation from H-37 to H-40 supported the relative assignment as shown. As illustrated by the data shown for the C-39 to C-40 rotamer, the homo- and heteronuclear couplings observed for this segment of etnangien methyl ester suggested a certain degree of flexibility. In particular, medium couplings from H-39 to H-40, H-39 to C-41, and from H-40 to Me-39 supported a certain degree of conformational flexibility. A relatively large heteronuclear coupling between H-39 and C-40 and a small coupling H-40 and C-38 in combination with these medium couplings indicated two interconverting conformers with *gauche* relationships of H-39 and 40-OH. Strong NOESY correlations, from H-37 to H-40 and from Me-39 to H₂-41, suggested a vicinity between these protons, which is explicable by the relative assignment, as shown (**3A**, **3B**).

For further clarification of this northern section, Rychnovsky's acetonide method was applied.¹³ Accordingly, the corresponding (38,40)- and (36,38)-acetonides **4** and **5** were prepared by treatment of the parent natural product with dimethoxypropane/ $TsOH$, as shown in Figure 3. They may be readily separated by HPLC. The (36,38)-acetonide **5** showed the characteristic ^{13}C NMR resonances for a 1,3-*syn*-diol derivative (i.e. 19.7 and 30.0 ppm for the acetonide-methyl groups). Furthermore, the all-*syn* relationship also between C-36, C-37, and C-38 was supported by a series of key NOESY correlations (from 37-H

(9) (a) Hoyer, T. R.; Hanson, P. R.; Vyvyan, J. R. *J. Org. Chem.* **1994**, *59*, 4096–4103. (b) Hoyer, T. R.; Zhao, H. *J. Org. Chem.* **2002**, *67*, 4014–4016.

(10) (a) Kouřimský, W.; Nanz, D. *J. Magn. Reson.* **2000**, *142*, 294–299. (b) Marquez, B. L.; Gerwick, W. H.; Williamson, R. T. *Magn. Reson. Chem.* **2001**, *39*, 499–530.

(11) For a recent review on novel methods for the stereochemical determination of complex polyketides, see: Menche, D. *Nat. Prod. Rep.* **2008**, *25*. In press: <http://dx.doi.org/10.1039/b707989n>.

(12) For a leading reference on J -based configurational analysis, also known as Murata's analysis, see: Matsumori, N.; Kaneno, D.; Murata, M.; Nakamura, H.; Tachibana, K. *J. Org. Chem.* **1999**, *64*, 866–876.

(13) (a) Rychnovsky, S. D.; Skalitzky, D. *J. Tetrahedron Lett.* **1990**, *31*, 945–948. (b) Evans, D. A.; Dale, L. R.; Gage, J. R. *Tetrahedron Lett.* **1990**, *31*, 7099–7100.

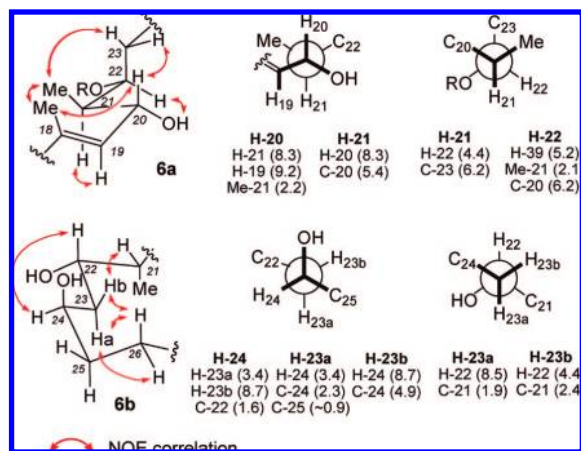


Figure 4. Rotamers determined for the C-18 to C-23 subunit (**6a**) and the C-21 to C-26 subunit (**6b**) of etnangien methyl ester (**2**); coupling constants $^3J_{H,H}$ and $^{2,3}J_{H,C}$ (Hz) in parentheses.

to 38-H and 36-H, from 37-H to 34-H₂, 1'a-H₃ to 38-H), as depicted. The (38,40)-acetonide **4**, in turn gave only two ^{13}C NMR resonances for the acetonide carbons, suggesting a twist conformation, which is indicative of a (38,40)-*anti* configuration. In addition, the 38,39-*anti* and 39,40-*syn* relationship was supported by the NOESY correlation between 38-H and 39-Me and 39-H and 40-H. With this additional stereochemical proof, the relative configuration of the northern part of etnangien (**1**) could be convincingly deduced as shown.

Relevant homo- and heteronuclear coupling constants and NOESY correlations for the C-19 to C-24 subunit **6** of etnangien methyl ester (**2**) are shown in Figure 4. A large homonuclear coupling between H-20 and H-21 and a small coupling from H-20 to Me-21 together with a large coupling from H-21 to C-20 indicated an antiperiplanar relationship between H-20 and H-21. In a similar fashion, an antiperiplanar relationship between H-19 and H-20 (i.e. by a large coupling between H-19 and H-20) and gauche relationships between H-21 and H-22 and between H-22 and Me-21 may be deduced (i.e. by small coupling from H-21 to H-22, and H-22 to Me-21 and large couplings from H-21 to C-23 and H-22 to C-38), suggesting that the C-5 to C-11 subunit resides in the depicted conformation **6a**. Four key NOESY correlations, from Me-18 to Me-21, H-19 to H-21, 20-OH to H-22 and Me-21 to H-23, supported the relative assignment as shown.

Determination of a relationship between the substituents at C-24 and C-22 relied on a confident assignment of the two diastereotopic protons H-23a and H-23b. A large homonuclear coupling between H-23a and H-22 together with small couplings from H-23a to C-24 and to C-25 and small couplings from H-23a to H-24 and to C-24 as well as to C-25 suggested that H-23a resides in an antiperiplanar conformation to H-22 and a gauche conformation to H-24. In the same way, an antiperiplanar relationship between H-23b and H-24 and a gauche situation from H-23b to H-22 was deduced by large couplings from H-23b to H-24 and to C-24 together with small couplings from H-23b to H-22 and C-21. These data suggest that the C-21 to C-25 subunit resides in the depicted conformation **6b**. Various NOESY correlations, i.e. from H-23a to H-26 and from H-23b to H-21 and to H-22, supported the relative assignment as shown.

Correlation of a relationship between the C-19 to C-24 and the C-35 to C-40 stereocenters **3** and **6** and determination of the macrocyclic stereocenter at C-28 could not be convincingly

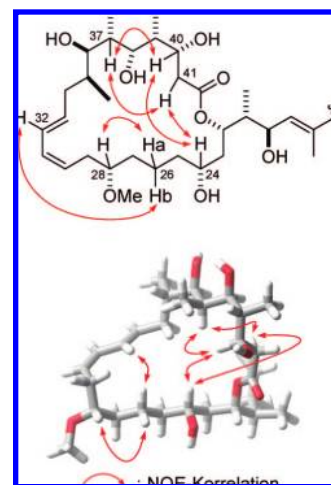


Figure 5. Perspective drawing of the lowest-energy conformation of etnangien methyl ester (**2**) generated by MacroModel v 8.5¹⁴ and selected transannular NOESY correlations (side chain omitted for reasons of clarity): assignment of the relative configuration of the macrocyclic core of etnangien.

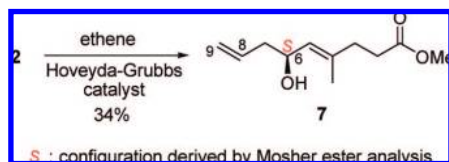
deduced by *J*-based configuration analysis. Therefore, 20,000-step Monte Carlo searches using MacroModel (version 8.5)¹⁴ with the MMFFS and the generalized Born/surface area (CB/SA) water solvent model¹⁵ were carried out on the possible stereochemical permutations to reveal a series of discrete families of low-energy conformations for the various stereoisomers within 10.00 kcal mol⁻¹ of the global minimum. The calculated dihedral angles for the lowest-energy conformation for **2** (see Figure 5) to the corresponding series of $^3J_{H,H}$ coupling constants, as determined by NMR, resulted in a close match, while for other stereochemical permutations, including the C-28 epimer, no apparent resemblances between spectral and calculated data were obtained. Furthermore, the conformation calculated for **2** accounted for a number of key transannular ROESY correlations (i.e., from H-24 to H-41, from H-26 to H-32, and from H-37 to H-41) allowing for a confident assignment of the relative configuration of the macrocyclic core of etnangien.

For further stereochemical proof, an array of conventional methods including derivatizations (Mosher ester analysis, selective protection of hydroxyls) and degradation (ozonolysis) was applied, both to etnangien and its methyl ester **2**. Under a variety of conditions, however, only complex product mixtures were obtained, which could not be separated into pure products using HPLC on various reverse and normal phases. Apparent obstacles were difficulties to selectively address one of the hydroxyls, in combination with the instability and structural complexity of these antibiotic agents. In particular, traces of acid or base led to complex product mixtures in all cases, and LC-MS analyses suggested isomerizations along the double bonds, eliminations, as well as translactonization and certain degrees of autoxidation, depending on the amount of oxygen present. These results were in agreement with stability tests of pure etnangien methyl ester in the presence of oxygen or light and in various pH buffers. Similarly, all attempts to oxidatively cleave olefinic double bonds of **2**, optionally with reductive workup, likewise only

(14) Mohamdi, F.; Richards, N. G. J.; Guida, W. C.; Liskamp, R.; Lipton, M.; Caufield, C.; Chang, G.; Hendrickson, T.; Still, W. C. *J. Comput. Chem.* **1990**, *11*, 440–467.

(15) Still, W. C.; Tempczyk, A.; Hawley, R. C.; Hendrickson, T. *J. Am. Chem. Soc.* **1990**, *112*, 6127–6129.

Scheme 1. Degradation of Etnangien Methyl Ester (**2**) by Olefin Cross-Metathesis in the Presence of Ethylene: Assignment of the Absolute Configuration at C-6 by Mosher Ester Analysis



produced intractable mixtures instead of expected dialdehyde or diol fragments.

We therefore turned our attention to an alternative approach, i.e. degradation under reductive conditions. Following a method recently introduced by the Höfle group, this involves cleavage of double bonds by olefin metathesis in the presence of ethylene.¹⁶ Notable advantages of this method are the very mild reaction conditions and the valuable option to start directly from the natural product. As shown in Scheme 1, using the Hoveyda–Grubbs ruthenium catalyst, a selective cleavage along the (8,9)-double bond could be effected, giving the side-chain fragment **7** in low yields. The constitution was readily confirmed by NMR spectral analyses, including ROESY and HMBC data. The absolute configuration at the isolated stereogenic center at C-6 could then be determined to be *S* by Mosher ester analysis, as depicted. Notably, this assignment is of critical importance as—in contrast to all other stereogenic centers—it may not be correlated to other stereogenic centers by *J*-based configuration analysis or modeling. Importantly, the same configuration was independently predicted by the bioinformatics approach, as discussed below. Therefore, it serves as an important internal standard for this more modern approach (*vide infra*).

Biosynthesis. In order to further confirm the stereochemical assignment, we then turned our attention to a complementary approach, which relies on the information available from the biosynthetic genes of etnangien and enables a configurational prediction of hydroxyl-bearing stereogenic centers. Biosynthetically, they are derived in a stereospecific fashion by ketoreductase (KR) mediated reduction of the corresponding ketones. Quite recently, the groups of Reid et al.¹⁷ and Caffrey et al.¹⁸ have studied in detail the core regions of these enzymes and proposed a model for the observed selectivity. Following this model, the configuration of the biosynthetically derived secondary alcohols may be determined in a simple fashion by analysis of the amino acid sequence in the core regions of these enzymes. In brief, the presence or absence of one amino acid, an aspartate residue, results either in *D*-configured alcohols (= B-type) or *L*-configuration (= A-type) in the absence of this amino acid. Importantly, the applicability of this method for configurational assignment of hydroxyl-bearing stereogenic centers has recently been proven in a number of cases.^{11,35} Indeed in all examples that correspond to myxobacterial metabolites, the absolute configuration of secondary hydroxyls was correctly predicted,^{11,35a,b} which corroborates the viability and applicability of this method for configurational assignment of hydroxyl-bearing stereogenic centers also for etnangien.

Accordingly, the biosynthetic gene cluster of etnangien (**1**) was studied in detail, revealing a highly complex and noncolinear polyketide synthase which is almost typical for myxobacterial secondary metabolism.¹⁹ We have cloned and identified the etnangien biosynthetic genes from *S. cellulosum* So ce56 within a functional genome project and reported the nucleotide sequence of the genes recently.²⁰ However, a *trans*-AT type and noncolinear assembly line was identified which made a prediction of the biosynthetic route hardly possible (see Figures 6 and 7). In the course of this study, a detailed bioinformatics-based analysis of the gene cluster was performed, revealing a likely biosynthetic scenario which could subsequently be used to predict the stereochemistry of the molecule by assigning each stereocenter to a respective biosynthetic module in the biosynthetic process. This model will be discussed in the following section.

The etnangien biosynthetic gene cluster belongs to the *trans*-AT type of polyketide synthases (PKS)^{21–23} because AT domains could not be identified within the PKS modules. Instead, two open reading frames encoding putative malonyl CoA-acyl carrier protein transacylases (*etnB* and *etnK*) are located upstream and downstream of the PKS genes. The gene product of *etnB* is most similar to malonyl CoA-acyl carrier protein transacylases from *Flavobacterium* sp. MED217 (33% identity and 51% similarity) and from *Bacillus halodurans* C-125 and *B. subtilis* subsp. *subtilis* str. 168 (32% identity and 52% similarity). The deduced amino acid sequence of EtnK contains two acyl transferase domains (NCBI Conserved Domain Search) and exhibits highest homology to the malonyl CoA-acyl carrier protein transacylases of *Pseudomonas fluorescens* Pf-5 (40% identity and 57% similarity) and MmpIII of *Burkholderia thailandensis* E264 (40% and 53%). *In silico* analysis of the substrate specificity of these AT domains identified malonyl-CoA as the preferred substrate for the second AT domain of EtnK with the active-site residues QQGHS LGR-FHNQV identified as highly similar to the characteristic motif QQGHS[L VIFAM]GR[FP]H[ANTGEDS][NHQ]V of other malonate specific AT domains.²⁴ The same motif was identified in the chivosazol biosynthesis protein ChiA that is assumed to transfer malonate units onto the ACPs of the chivosazol *trans*-AT PKS²¹ and within the LnmG AT of the leinamycin biosynthetic gene cluster which was biochemically shown to load all six ACPs of the corresponding assembly line with malonyl-CoA.²⁵ The substrate specificity of the two additional AT domains can currently not be predicted. However, as it is assumed that the biosynthesis starts by the loading of succinate to the first ACP of module 1 in EtnD (see Figure 6), one of these AT domains might be responsible for this step. The function of the third AT domain is currently obscure. Next, the incorporation of the methyl group at C4 may well be carried out by an HMG-CoA-like mechanism. Recently, it has been

- (16) (a) Karama, U.; Höfle, G. *Eur. J. Org. Chem.* **2003**, 1042–1049. (b) Niggemann, J.; Bedorf, N.; Flörke, U.; Steinmetz, H.; Gerth, K.; Reichenbach, H.; Höfle, G. *Eur. J. Org. Chem.* **2005**, 5013. (c) Jundt, L.; Steinmetz, H.; Luger, P.; Weber, M.; Kunze, B.; Reichenbach, H.; Höfle, G. *Eur. J. Org. Chem.* **2006**, 5036.
- (17) Reid, R.; Piagentini, M.; Rodriguez, E.; Ashley, G.; Viswanathan, N.; Carney, J.; Santi, D. V.; Hutchinson, C. R.; McDaniel, R. *Biochemistry* **2003**, *42*, 72–79.
- (18) Caffrey, P. *ChemBioChem* **2003**, *4*, 654–657.

- (19) For a recent review on the biosynthesis of myxobacterial metabolites, see: (a) Wenzel, S. C.; Müller, R. *Nat. Prod. Rep.* **2007**, *24*, 1211–1224.
- (20) Schneiker, S.; et al. *Nat. Biotechnol.* **2007**, *25*, 1281–1289.
- (21) Perlova, O.; Gerth, K.; Kaiser, O.; Hans, A.; Müller, R. *J. Biotechnol.* **2006**, *121*, 174–191.
- (22) (a) Piel, J.; Hui, D.; Fusetani, N.; Matsunaga, S. *Environ. Microbiol.* **2004**, *6*, 921–928. (b) Shen, B. *Curr. Opin. Chem. Biol.* **2003**, *7*, 285–295.
- (23) Wenzel, S. C.; Müller, R. *Curr. Opin. Chem. Biol.* **2005**, *9*, 447–458.
- (24) Yadav, G.; Gokhale, R. S.; Mohanty, D. *J. Mol. Biol.* **2003**, *328*, 335–363.
- (25) Cheng, Y.-Q.; Tang, G.-L.; Shen, B. *Proc. Natl. Acad. Sci. U.S.A.* **2003**, *100*, 3149–3154.

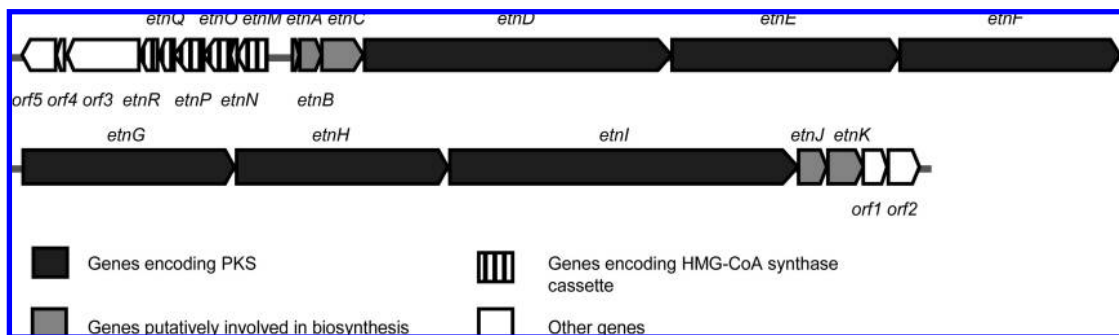


Figure 6. Physical map of the chromosomal region containing the etnangien biosynthetic genes.

demonstrated that HMG-CoA synthases (encoded here by *etnO*) and associated ACPs (acyl carrier protein encoded by *etnM*), KS-like decarboxylases (KS^S encoded by *etnN*) and two enoyl-CoA hydratase-like enzymes (encoded by *etmP* and *etmQ*) can insert methyl groups (“ β -branches”) into growing polyketide chains as shown in Figures 7 and 8.²⁶ The resulting intermediate is then transferred to module 2, and subsequently modules 3–5 (KS-DH-KR-ACP) catalyze the incorporation and modification of further acetate units derived from malonyl-CoA resulting in the formation of double bonds. Module 6 again seems to function in cooperation with the HMG-CoA synthase plus modifying enzymes and is thus most likely involved in the methylation at C18. The intermediate one would predict for the PKS assembly line in module 6 is shorter than the expected substrate for methylation as shown in Figure 6. We speculate that this discrepancy can be explained by programmed iteration of one of the modules 2–5 which would result in the incorporation of additional malonyl-CoA units into the growing chain. Similar scenarios for programmed iteration of one module have been described for the stigmatellin, borrellidin, aureothin, and DKxanthene PKSs, respectively.^{23,27,28}

Further assembly is carried out by modules 7–10, which catalyze the condensation of four additional malonyl-CoA units. Interestingly, the expected ER domain in module 10 is missing. However, an ER domain could be identified in module 16 which might be involved in enoyl reduction in this position. Next, the biosynthesis seems to continue on module 12 (although the KS domain of module 11 shows all conserved residues and skipping²⁹ of module 11 is hardly explainable, see below). Module 12 contains a methyltransferase domain similar to the one found in melithiazol biosynthesis³⁰ and is assumed to methylate the β -keto-intermediate giving rise to C28. The incorporation of further malonyl-CoA units is most likely carried out by modules 13 and 15–19. We assume that modules 11, 14, and 20 are skipped (although there is no indication for their

inactivity from sequence analysis alone; *vide infra*). If this assumption is correct, DH activities are missing in modules 13 and 15, whereas DH domains were identified within modules 16 and 18. The latter domains are not required for the respective reduction steps and might thus be complementing the missing domains.

In addition to these irregularly distributed domains the etnangien biosynthetic assembly framework includes unusual split modules (module 4, 7, 10, and 14) which seem to be characteristic for myxobacteria¹⁹ and were in fact described in these bacteria first.³¹ Recently, such disrupted modules have also been found in the bacillaene biosynthetic assembly line in which—much as suggested here for module 12 and 13—a *cis*-double bond coincides with the disrupted module.³²

To further verify the proposed function of the HMG-CoA synthase cassette in etnangien biosynthesis, we aimed to inactivate the corresponding core gene. Mutants were generated by integration of a hygromycin resistance cassette via homologous recombination into *etnP*. After genetic verification of the mutants, the phenotypes were compared to the wild type, showing that the mutants lost their ability to produce etnangien (see Supporting Information) which demonstrates that EtnP is indeed required for etnangien biosynthesis.

As described above, the etnangien gene cluster belongs to the family of *trans*-AT PKS. Recently, numerous studies showed that such megasynthases exhibit many exceptions from the textbook rules of PKS biosynthesis.³³ In a recent study, phylogenetic analysis of such PKSs³⁴ suggests that *trans*-AT PKSs have evolved independently from *cis*-AT PKSs. In addition to the unique acyl transfer mechanism, the enzymes exhibit highly aberrant architectures with modules carrying novel catalytic domains or domain orders or modules having no apparent function or relation to the polyketide structure. From this analysis, it seems possible to predict the structure of the secondary metabolite based on *in silico* analysis alone because the substrate specificity for each KS can theoretically be predicted.³⁴ We thus aimed to compare the KSs from the etnangien PKS with other *trans*-AT KSs and analyzed whether

- (26) (a) Calderone, C. T.; Kowtoniuk, W. E.; Kelleher, N. L.; Walsh, C. T.; Dorrestein, P. C. *Proc. Natl. Acad. Sci. U.S.A.* **2006**, *103* (24), 8977–8982. (b) Gu, L.; Jia, J.; Liu, H.; Hakansson, K.; Gerwick, W. H.; Sherman, D. H. *J. Am. Chem. Soc.* **2006**, *128*, 9014–9015. (c) Simunovic, V.; Müller, R. *ChemBioChem* **2007**, *8*, 497–500. (d) Simunovic, V.; Müller, R. *ChemBioChem* **2007**, *8*, 1273–1280.
- (27) Moss, S. J.; Martin, C. J.; Wilkinson, B. *Nat. Prod. Rep.* **2004**, *21*, 575–593.
- (28) Meiser, P.; Weissman, K. J.; Bode, H. B.; Dickschat, J. S.; Sandmann, A.; Müller, R. *Chem. Biol.* **2008**, *15*, 771–781.
- (29) (a) Thomas, I.; Martin, C. J.; Wilkinson, C. J.; Staunton, J.; Leadlay, P. F. *Chem. Biol.* **2002**, *9*, 781–787. (b) Wenzel, S. C.; Meiser, P.; Binz, T. M.; Mahmud, T.; Müller, R. *Angew. Chem., Int. Ed.* **2006**, *45*, 2296–2301.
- (30) Weinig, S.; Hecht, H.-J.; Mahmud, T.; Müller, R. *Chem. Biol.* **2003**, *10*, 939–952.

- (31) Silakowski, B.; Nordsiek, G.; Kunze, B.; Blöcker, H.; Müller, R. *Chem. Biol.* **2001**, *8*, 59–69.
- (32) (a) Butcher, R. A.; Schroeder, F. C.; Fischbach, M. A.; Straight, P. D.; Kolter, R.; Walsh, C. T.; Clardy, J. *Proc. Natl. Acad. Sci. U.S.A.* **2007**, *104* (5), 1506–1509. (b) Moldenhauer, J.; Chen, X.-H.; Borriss, R.; Piel, J. *Angew. Chem., Int. Ed.* **2007**, *46*, 8195–8197.
- (33) (a) Kopp, M.; Irschik, H.; Pradella, S.; Müller, R. *ChemBioChem* **2005**, *6*, 1277–1286. (b) Piel, J. *Proc. Natl. Acad. Sci. U.S.A.* **2002**, *99*, 14002–14007.
- (34) Nguyen, T.; Ishida, K.; Jenke-Kodama, H.; Dittmann, E.; Gurgui, C.; Hochmuth, T.; Taudien, S.; Platzer, M.; Hertweck, C.; Piel, J. *Nat. Biotechnol.* **2008**, *26*, 225–233.

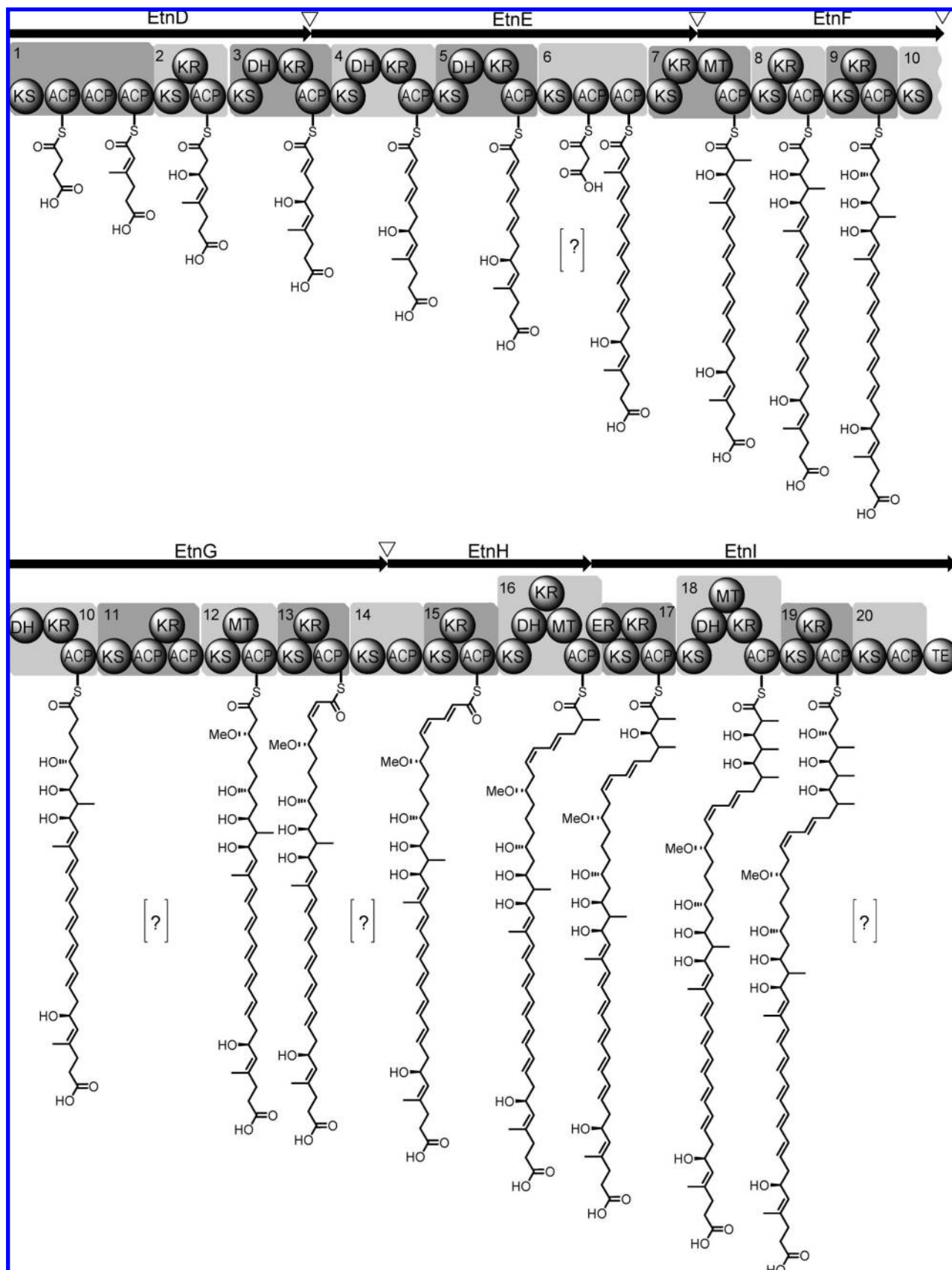


Figure 7. Etnangien biosynthetic assembly line from *Sorangium cellulosum*. Corresponding genes are depicted as black arrows. Triangles show the split modules in the assembly line. Shaded boxes indicate the modules; spheres indicate the catalytic domains. Question marks indicate modules in which KS domains are thought to be inactive, resulting in lack of chain extension (“skipping”). The intermediate predicted for module 6 is shorter than the expected substrate for methylation as shown, which may be explained by programmed iteration of one of the modules 2–5 (see text). Abbreviations for the domain designation: KS - β -ketoacyl synthase; ACP - acyl carrier protein; KR - β -ketoacyl reductase; DH - dehydratase; MT - methyltransferase; TE - thioesterase.

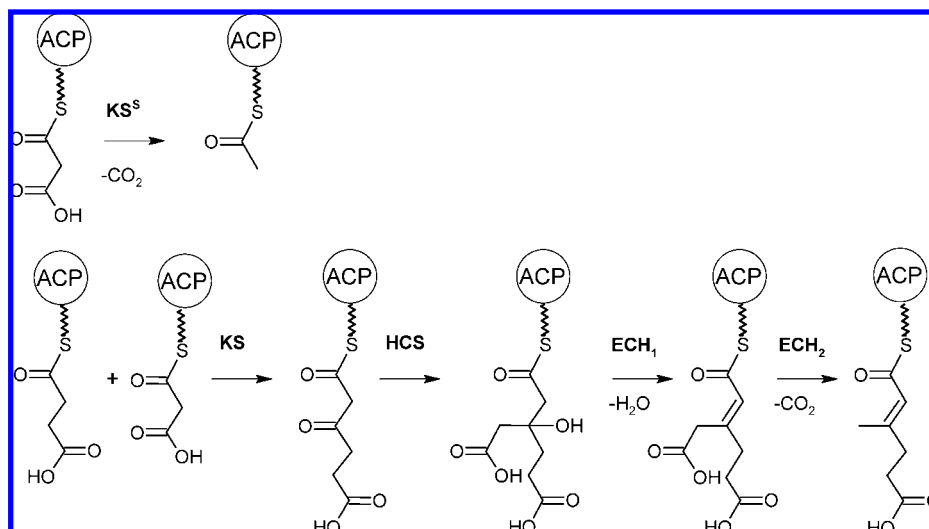


Figure 8. Proposed function of the HMG-CoA synthase (HCS) and modifying enzymes in the methylation of the etnangien intermediates.

this phylogenetic analysis would help to predict the highly unusual biosynthetic pathway leading to etnangien. The results compare reasonably well with our biosynthetic hypothesis presented in Figure 7 (see also Supporting Information). In general, the intermediates shown are in accordance with the prediction of each intermediate obtained by the analysis based on substrate specificity of the KS domains from *trans*-AT PKSs. Although module skipping is expected to occur in our biosynthetic hypothesis, none of the analyzed etnangien KSs belong to the phylogenetic clade including the non-elongating KSs, and therefore, it was not possible to confirm our assumption regarding the skipping of some modules (see above and Figure 7). Such non-elongating KS domains usually lack some of the conserved residues required for activity. However, the alignment of all etnangien KS domains showed that all conserved amino acid residues required for the decarboxylation and condensation activity are present in these domains, raising the question how and why skipping occurs in the etnangien megasynthetase.

Another interesting finding is the predicted substrate specificity of KS1. We assume that succinate is the starter unit of etnangien biosynthesis. However, the phylogenetic analysis showed that KS1 belongs to clade IV-harboring domains accepting substrates exhibiting β -OH groups. Thus, the real starter unit of etnangien biosynthesis currently remains elusive.

In summary, etnangien biosynthesis exhibits one of the most obscure examples of polyketide megasynthetase architecture reported to date. The prediction of the chemical compound formed by this PKS would have been almost impossible based on *in silico* analysis, even using the most sophisticated technology available today.³⁴ However, by using the basic structural information available it was possible to develop a reasonable biosynthetic scheme and use this analysis to predict the stereochemistry of each stereocenter within the molecule from the molecular architecture of the megasynthetase (*vide infra*).

During the biosynthetic process the KR domains generate hydroxyl groups with different stereochemical configuration,

either *D* or *L*. Subsequent elimination of water results in either *cis* or *trans* double bonds, depending on the stereochemistry of the preceding intermediate. Analysis of the respective ketoreductase core regions by the method of Reid and Caffrey^{17,18,35} revealed aspartic acid residues in the KR core region for alcohols at C6, C20, C22, C36, C38, as shown in Table 2. Correspondingly, the absence of this amino acid in modules 11, 13, and 19 suggested these hydroxyl-bearing stereogenic centers to be *L*-configured.

As shown in the figure in Table 2, comparing these data to the configurations independently derived by our more conventional approach as discussed above, resulted in a perfect match, which validates our previous assignment and vice versa. Again, this also proves the viability of such a bioinformatics approach to configurational assignment.

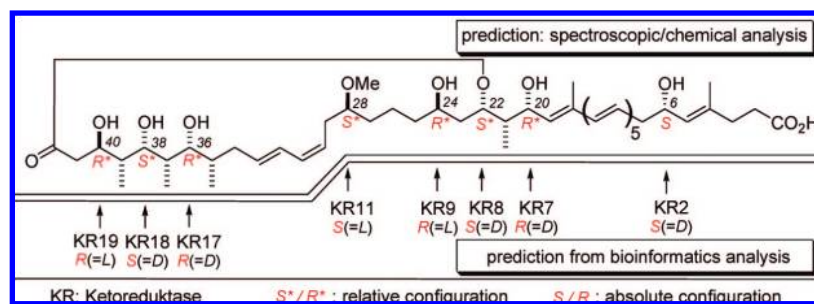
Importantly, the absolute configurations of all seven stereogenic centers in the macrocyclic core as obtained by this genetic analysis of the corresponding KR core regions were in complete agreement with the relative assignment obtained above. Therefore, the absolute configuration of the macrolide portion of etnangien could be predicted with very good confidence, as depicted. Notably, the configuration of side-chain center (C-6), which was firmly established by chemical methods (see above), was correctly predicted also, which further corroborates the viability of this approach. In addition, also the assignment of the double bond stereochemistry is in perfect agreement with the prediction derived from KR domain analysis (see Table 2).

Figure 9 summarizes the assignment of the full relative and absolute configuration for etnangien. The full stereochemical assignment of the polyketide macrolide is proposed as **8** (*4E,6S,8E,10E,12E,14E,16E,18E,20R,21R,22S,24R,28S,30Z,32E,-35S,36R,37S,38S,39R,40R*).

Conclusion

In summary, we have developed a potent novel and stable analogue of the myxobacterial RNA polymerase inhibitor etnangien (**1**), the methyl ester **2**. The preparation of this compound was efficiently enabled by direct esterification of the parent natural antibiotic in the crude extract obtained after fermentation of *S. cellulosum* So ce1045. Etnangien methyl ester is readily isolated by a simple purification protocol and is stable in solution under neutral conditions. It shows similar antibacte-

(35) (a) Janssen, D.; Albert, D.; Jansen, R.; Müller, R.; Kalesse, M. *Angew. Chem., Int. Ed.* **2007**, *46*, 4898–4901. (b) Udway, D. W.; Zeigler, L.; Asolkar, R. N.; Singan, V.; Lapidus, A.; Fenical, W.; Jensen, P. R.; Moore, B. S. *Proc. Natl. Acad. Sci. U.S.A.* **2007**, *104*, 10376. (c) Bock, M.; Buntin, K.; Müller, R.; Kirschnig, A. *Angew. Chem., Int. Ed.* **2008**, *47*, 2308–2311.

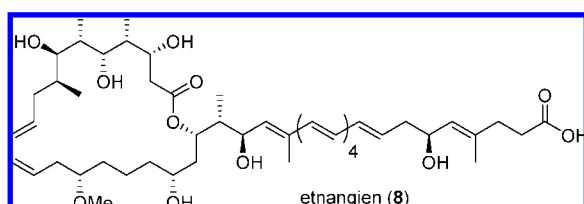
Table 2. Proposed Configurations of the Hydroxyl-Bearing Stereogenic Centers of Etnangien by Analysis of the Corresponding Ketoreductase Core Regions, in Comparison to the Assignment by Spectroscopic and Chemical Methods

ketoreductase	diagnostic Asp region	alcohol stereochemistry	double bond
KR2	AGVLRDG-FIVRKQ	B-type (D,S), (C-6)	—
KR3	AGVLQDS-FVFNKT	B-type (D)	<i>trans</i>
KR4	AGVLQDS-FVFNKT	B-type (D)	<i>trans</i>
KR5	AGVVEDS-FLVRKT	B-type (D)	<i>trans</i>
KR7	PLVLSDR-SLARME	B-type (D,R), (C-20)	—
KR8	AGTTRDA-LLPRKT	B-type (D,S), (C-22)	—
KR9	AGVESGG-ALLDKR	A-type (L,R), (C-24)	—
KR10	AGVLRDS-TIAKKT	B-type —	—
KR11	AGVESGG-ALLDKR	A-type (L,S), (C-28)	—
KR13	AGNTDFTNPAFVRKT	A-type (L)	<i>cis</i>
KR15	AGVTRDA-LLLHKT	B-type (D)	<i>trans</i>
KR16	AIVLRDR-SLREMD	B-type —	—
KR17	AVGTFDK-SVANTT	B-type (D,R), (C-36)	—
KR18	AVGTFDK-SVANTT	B-type (D,S), (C-38)	—
KR19	AGVESGG-AVVDRS	A-type (L,R), (C-40)	—

rial potency as compared to that of etnangien which suggests that a free acid is not essential for biological activity. These results demonstrate that it is possible to modify and stabilize the etnangien structure, yet still retain activity. Furthermore, the full stereostructure of etnangien (**1**) was determined by a combination of high-field NMR method, including Murata's method of *J*-based configurational analysis, chemical degradation, molecular modeling and genetic methods, relying on the development of a biosynthetic model based on a complex megasynthetase. Etnangien biosynthesis is directed by a highly unusual *trans*-AT polyketide synthase exhibiting a number of nontextbook features including split module organization, programmed iteration, methyl branch incorporation via a HMG-CoA-synthase box plus an uncommon starter unit. Biosynthetic analysis and chemical methods proposed the same configurations for the individual stereogenic centers of etnangien, providing a structure with good confidence. Confirmation of this proposal will require a stereocontrolled total synthesis of etnangien. In general, it is expected, that these findings will advance the further development of the etnangiens as promising structurally novel antibiotic lead structures.

Experimental Section

Preparation of Etnangien Methyl Ester (2). A 70-L fermentation batch of strain So ce1045, cultivated at the HZL,⁷ was grown in a medium named "1045-2-1",⁷ containing soluble starch, 0.25%;

**Figure 9.** Absolute and relative configuration of etnangien.

insoluble starch (Cerestar), 0.25%; peptone from soy meal, 0.3%; soy meal, defatted, 0.05%; CaCl₂ 2H₂O, 0.1%; and Na-Fe-EDTA, 8 mg/L, in the presence of 1% (v/v) of Amberlite XAD-16 adsorber resin at 30 °C for eight days. After harvesting by centrifugation, the mixture of wet cell mass and adsorber resin (350 g) was thoroughly extracted (as controlled by analytical HPLC) with three batches of each 2 L of methanol. The extract was concentrated on a rotary evaporator at 30 °C/50 mbar to the water phase. After acidification with NH₄OAc and HOAc to pH 5, the aqueous phase (1 L) was extracted with one portion of 1.5 L and two portions of 1 L of ethyl acetate. The combined organic phase was evaporated at 30 °C/150 mbar to give a crude oil (14 g), which was directly dissolved in methanol for storage at -78 °C. For esterification, a solution of 500 mg of the crude oil in 1 mL diethyl ether/methanol = 9:1 was prepared and treated at 0 °C with a solution of diazomethane in ether, which was prepared as previously described from 1-methyl-3-nitro-1-nitroguanidine³⁶ and washed with pH 9 buffer immediately prior to addition. After 8 min, the reaction was stopped by addition of pH 5 buffer (1 mL). The organic phase was separated, and the aqueous phase was thoroughly extracted with ethyl acetate. After drying (MgSO₄), and evaporation of the organic phase, the residue was purified by flash chromatography on silica gel (dichloromethane/methanol = 12:1 to 10:1) and subsequent preparative RP HPLC on Nucleodur C18 (column 250 mm × 21 mm, 7 μm, flow 18 mL/min, detection: UV absorption at 365 nm, solvent: methanol/water = 79:21) to give etnangien methyl ester (**2**) (10 mg). Colorless amorphous solid; [α]_D²² +17.4° (c 0.38, MeOH); IR (film) ν_{max} 3018, 2967, 1715, 1094 cm⁻¹; UV(MeOH) λ_{max} 375, 355, 338, 323, 226, 235 nm; NMR data: see Supporting Information; HRESI(+)MS 877.5443 [(M + Na)⁺, C₅₀H₇₈O₁₁Na requires 877.5442].

Preparation of Etnangien (1) from Etnangien Methyl Ester (2). A solution of **2** (2.00 mg, 2.34 μmol) in 1 mL DMSO/water = 1:3 was treated under argon at room temperature with 5 mg porcine liver esterase (Sigma) and stirred for 24 h. Etnangien (**1**) (1.10 mg, 1.31 μmol, 56%) was recovered from the crude mixture using

(36) McKay, A. F. *J. Am. Chem. Soc.* **1948**, *70*, 1974.

previously established protocols.⁷ The spectroscopic and physico-chemical properties were identical to those reported previously.⁷

Degradation of Etnangien Methyl ester (2) by Cross Metathesis with Ethylene. Etnangien methyl ester (**2**, 5.3 mg, 6.2 μmol) and Hoveyda–Grubbs catalyst (1.6 mg, 2.4 μmol) were dissolved in dried dichloromethane (10 mL). The atmosphere above the light-green solution was then replaced with ethylene. After stirring for 4 h, the solvent was evaporated *in vacuo*. Purification of the residue by preparative HPLC (hexane/ethyl acetate = 3:1) gave degradation product **7** (420 μg , 2.12 μmol , 34%) as a colorless oil. R_f = 0.33 (hexanes/EtOAc = 3:1); $[\alpha]_D^{23}$ = +1.1 (*c* 1.0, CHCl_3); $^1\text{H NMR}$ (300 MHz, CDCl_3) δ 1.70 (d, J = 1.3 Hz, 3H), 2.24–2.36 (m, 4H), 2.42–2.48 (m, 2H), 3.67 (s, 3H), 4.41 (ddd, J = 7.0 Hz, J = 7.0 Hz, J = 7.0 Hz, 1H), 5.10–5.17 (m, 2H), 5.23 (dq, J = 8.4 Hz, J = 1.3, 1H), 5.79 (dddd, J = 17.1 Hz, J = 10.1 Hz, J = 7.1 Hz, J = 7.1 Hz, 1H), $^{13}\text{C NMR}$ (75 MHz, CDCl_3) δ 16.6, 32.6, 34.3, 42.1, 51.6, 67.5, 118.0, 127.7, 134.3, 136.9, 173.5; HRMS calculated for $\text{C}_{11}\text{H}_{18}\text{O}_3$: 198.1256, found: 198.1253.

Inactivation of the HMG-CoA Synthase Encoding Gene. Primers OP158 (5'-agatctCGGAGAAGGATCGTATCGAG-3') and OP159 (5'-aagcttCGAGCCGTACGAGAAATACC-3') were used for generation of an inactivation fragment (inserted restriction sites are indicated in lower case). A PCR product containing the HMG-CoA synthase-encoding fragment was obtained from the chromosome of *S. cellulosum* So ce56 and was cloned into a pSUP102 derivative as described previously⁷ to generate plasmid pOPB158. Plasmid pOPB158 was introduced into So ce56 by conjugational

transfer.⁷ Verification of the mutants and product analysis was performed as described recently.²⁰

Acknowledgment. This work was generously supported by the Fonds der Chemischen Industrie (Liebig-Stipendium to D.M., Doktorandenstipendium to F.A.), the Deutsche Forschungsgemeinschaft, the HGF (postdoctoral stipend to N.H.) and the Wild-Stiftung. We thank the HZI for support and Jorma Hassfeld for fruitful suggestions. Furthermore, we thank Teresa Carlomagno and Christophe Farès (both Max Planck Institute for Biophysical Chemistry, Göttingen) for measurement of HSQC-HECADE spectra, Tatjana Arnold, Antje Ritter and Kerstin Schober (all HZI, Braunschweig) for technical support, and the fermentation group of the HZI for support with large-scale fermentation. Research in R.M.'s laboratory was funded by the Bundesministerium für Bildung und Forschung (BMB+F).

Supporting Information Available: Experimental procedures, tables of spectral and calculated data and copies of 1D and 2D NMR spectra for compounds **1**, **2**, **4**, **5**, and **7**. HPLC–MS analysis of the HMG-CoA synthase negative mutant in comparison to the wild-type and predicted functions of proteins involved in etnangien biosynthesis in *Sorangium cellulosum* So ce56. Complete reference 20. This information is available free of charge via the Internet at <http://pubs.acs.org>.

JA804194C